1990-03

Boundary layer structure of an explosive cyclone

Steeley, Glen D.

Monterey, California. Naval Postgraduate School

(2)

NAVAL POSTGRADUATE SCHOOL
Monterey, California

THESIS

BOUNDARY LAYER STRUCTURE OF AN EXPLOSIVE CYCLONE

by

Glen D. Steeley

March 1990

Thesis Advisor W. A. Nuss

nclassified

curity classification of this page

REPORT DOCUMENTATION PAGE

a Report Security Classification Unclassified		1b Restrictive Markings	
2a Security Classification Authority		3 Distribution Availability of Report	
2b Declassification Downgrading Schedule		Approved for public release; distribution is unlimited.	
4 Performing Organization Report Number(s)		5 Monitoring Organization Report Number(s)	
6a Name of Performing Organization Naval Postgraduate School	6b Office Symbol (if applicable) 35	7a Name of Monitoring Organization Naval Postgraduate School	
6c Address (city, state, and ZIP code) Monterey, CA 93943-5000		7b Address (city, state, and ZIP code) Monterey, CA 93943-5000	
8a Name of Funding Sponsoring Organization	8b Office Symbol (if applicable)	9 Procurement Instrument Identification Number	
8c Address (city, state, and ZIP code)		10 Source of Funding Numbers	
		Program Element No	Project No / Task No / Work Unit Accession No

11 Title (include security classification) BOUNDARY LAYER STRUCTURE OF AN EXPLOSIVE CYCLONE

12 Personal Author(s) Glen D. Steeley

13a Type of Report	13b Time Covered	14 Date of Report (year, month, day)	15 Page Count
Master's Thesis	From To	March 1990	35

16 Supplementary Notation The views expressed in this thesis are those of the author and do not reflect the official policy or position of the Department of Defense or the U.S. Government.

17 Cosati Codes			18 Subject Terms (continue on reverse if necessary and identify by block number)
Field	Group	Subgroup	Meteorology, explosive cyclogenesis, ERICA.

19 Abstract (continue on reverse if necessary and identify by block number)

A detailed analysis of the horizontal boundary layer structure of the warm front of an open ocean explosive cyclone in Intensive Observation Period (IOP) 2 of the Experiment on Rapidly Intensifying Cyclones in the Atlantic (ERICA) is conducted. Data for this study consists of aircraft data averaged over one minute supplimented by satellite and drifting buoy observations. Analysis of surface winds and fluxes was done using the Brown-Liu Marine PBL model. Results show a PBL which differs from that found in typical cyclones, with large latent heat fluxes south of the warm front and with relatively weak sensible heat fluxes about the warm front. Boundary layer stratification was stable north of the warm front and unstable south of the warm front. A mechanism for moist frontogenesis is proposed whereby the destabilizing effects of the latent heat flux enhances frictional convergence along the warm front. These fluxes warm and moisten the cyclone's warm sector, enhancing unstable convection along the warm front and thereby enhancing the vertical motion. This enhanced vertical motion would strengthen the geostrophic deformation of the θ_v gradient and potentially enhance cyclogenesis.

theta sub epsilon

20 Distribution Availability of Abstract	21 Abstract Security Classification	
☒ unclassified unlimited ☐ same as report ☐ DTIC users	Unclassified	
22a Name of Responsible Individual W. A. Nuss	22b Telephone (include Area code) (408) 646-2044	22c Office Symbol 63Nu

DD FORM 1473,84 MAR 83 APR edition may be used until exhausted
All other editions are obsolete

security classification of this page

Unclassified

Approved for public release; distribution is unlimited.

Boundary Layer Structure of an
Explosive Cyclone

by

Glen D. Steeley
Lieutenant, United States Navy
B.A., University of Washington, 1982

Submitted in partial fulfillment of the
requirements for the degree of

MASTER OF SCIENCE IN METEOROLOGY AND PHYSICAL OCEANOGRAPHY

from the

NAVAL POSTGRADUATE SCHOOL
March 1990

Author: 

Glen D. Steeley

Approved by: 

W. A. Nuss, Thesis Advisor

K. L. Davidson, Second Reader

R. J. Renard, Chairman,
Department of Meteorology

ABSTRACT

A detailed analysis of the horizontal boundary layer structure of the warm front of an open ocean explosive cyclone in Intensive Observation Period (IOP) 2 of the Experiment on Rapidly Intensifying Cyclones in the Atlantic (ERICA) is conducted. Data for this study consists of aircraft data averaged over one minute supplimented by satellite and drifting buoy observations. Analysis of surface winds and fluxes was done using the Brown-Liu Marine PBL model. Results show a PBL which differs from that found in typical cyclones, with large latent heat fluxes south of the warm front and with relatively weak sensible heat fluxes about the warm front. Boundary layer stratification was stable north of the warm front and unstable south of the warm front. A mechanism for moist frontogenesis is proposed whereby the destabilizing effects of the latent heat flux enhances frictional convergence along the warm front. These fluxes warm and moisten the cyclone's warm sector, enhancing unstable convection along the warm front and thereby enhancing the vertical motion. This enhanced vertical motion would strengthen the geostrophic deformation of the θ_e gradient and potentially enhance cyclogenesis.

TABLE OF CONTENTS

I. INTRODUCTION.

Maritime explosive cyclogenesis poses a problem for mariner and meteorologist alike with its unpredictable sudden severe weather. Explosive cyclogenesis is defined as a central pressure drop of 24 mb in 24 hours at 60°N, geostrophically adjusted for other latitudes by multiplying the deepening rate by $\left(\frac{\sin \theta}{\sin 60^\circ} \right)$ (Sanders and Gyakum 1980).

Forecasting explosive cyclogenesis is difficult due to incomplete understanding of the triggering mechanisms that distinguish it from non-explosive development. It has been shown that both upper level and boundary layer dynamics contribute to explosive development but their relative importance and the extent to which they interact is unclear. It is most probable that explosive cyclogenesis has no single trigger but is rather the result of one of many possible combinations of forcing mechanisms. The upper level influences on explosive development are best known and include enhanced cyclonic vorticity advection due to subsidence induced vortex tube stretching (Boyle and Bosart 1986) and enhanced frontal vertical circulation due to jet streak interaction with surface baroclinicity (Uccellini et.al. 1984).

The role of boundary layer processes in explosive development is less understood, but preliminary investigations have focused on surface fluxes of heat and moisture as forcing mechanisms. Sanders and Gyakum (1980) showed that explosive cyclones were winter events with a strong preference for development over the warm waters of the Kuroshio current east of Japan and the Gulf Stream current east of the United States. This relationship suggests that heat and moisture fluxes resulting from air-sea temperature differences are a factor in explosive development. Observational evidence for the influence of surface heat fluxes on explosive cyclogenesis was provided by Davis and Emanual (1988) in their investigation on the propensity of the Limited-area Fine-mesh Model (LFM) to underpredict rapid maritime cyclogenesis. Their hypothesis was that the model failed to account for warming due to surface heat and moisture fluxes. Twenty nine cases of explosive storms off the east coast of the United States were examined and in all cases the difference between predicted and actual development could be associated with the occurrence of warming due to surface fluxes. A concurrent climatological study of the same region from 1963-1977 showed a strong correlation between regions of large sea-surface fluxes and regions of explosive cyclogenesis.

While emphasizing atmospheric warming due to surface fluxes, Davis and Emanuel (1988) did not explicitly define the flux contribution to cyclogenesis. Their contention was that surface heating acts to raise 1000-500 mb thickness towards a potential thickness defined by the sea-surface temperature. To achieve this thickness increase the surface fluxes must directly feed the ascending air of a cyclone. Other studies suggest mechanisms other than the fluxes are responsible for this atmospheric warming. Kuo and Reed (1988), for example, concluded that surface fluxes played a minimal role in one case of explosive cyclogenesis. Although they found that condensational heating associated with areas of heavy precipitation led to rapid development through enhanced latent heat release, the surface heat and moisture fluxes contributed very little to this latent heat release. The differing impacts of the fluxes may be due to details in the distribution of surface fluxes and boundary layer processes in developing cyclones.

The distribution of surface fluxes in west coast non-explosive mid-latitude storms was examined by Fleagle and Nuss (1985) as part of the Storm Transfer and Response Experiment (STREX). Surface fluxes were found to have relatively large positive values in the cold sector behind the cold front but small or negative values in a 200 km region of the warm sector in advance of the cold front. This distribution of surface fluxes would act to oppose cyclogenesis by reducing the baroclinicity of the cyclone through the warming of the cold air behind the cold front.

This negative effect of the fluxes on cyclogenesis differs substantially from Bosart and Lin's (1984) examination of the 1979 President's Day storm, which suggested a more positive role of surface fluxes in explosive cyclogenesis. In this particular case, a cyclone developed explosively after moving offshore over the Gulf Stream in the vicinity of Cape Hatteras. They concluded that surface sensible heat fluxes ahead of the surface low acted to pre-condition the environment by enhancing the low-level baroclinic zone. Numerical model studies by Uccellini et al (1987) confirm the significant role of fluxes in fostering explosive development of this cyclone. The distribution of surface heating and moistening in this case increased low-level frontogenesis as well as directly feeding the regions of latent heat release in the mid-troposphere.

Nuss (1989) examined the relationship between flux distribution and cyclogenesis through a series of numerical simulations using identical initial atmospheric conditions but different surface fluxes and sea-surface temperature distributions. The control case for this experiment used a zonal SST distribution with upward heat and moisture fluxes to the west of the surface low and downward fluxes to the east, which is similar to flux distributions of west coast systems. A simulation using a sinusoidal SST distribution

was then run which produced additional upward fluxes to the northeast of the surface low, similar to the Presidents' Day storm. A comparison of simulation results after 24 hours showed that the second case deepened more rapidly than the control (1.65 mb h^{-1} vice 1.47 mb h^{-1}). The control case showed large upward fluxes in the cold sector behind the cold front and near zero fluxes in the warm sector in front of the cold front. In contrast, the second case had large upward fluxes not only in the cold sector but also to the northeast of the surface low in advance of the warm front. Additionally, a small upward flux was found throughout the warm sector. The increased deepening rate for the second case was attributed to the destabilizing effects of upward fluxes of heat and moisture on the boundary layer which resulted in increased downward momentum fluxes to the north of the warm front. This in turn enhanced the associated frontal ageostrophic secondary circulation, leading to increased frontal convergence and vertical circulations. Cyclogenesis was then enhanced through an associated increase in the release of latent heat.

These studies indicate that the planetary boundary layer (PBL) and frontal structure associated with cyclones has the following attributes:

- A strong, stable capping inversion above a well mixed boundary layer in the cold region behind the cold front and in advance of the warm front;
- Weak or neutral stratification in the warm sector and unstable stratification in the cool sectors of a cyclone;
- A narrow updraft of warm air above the surface cold and warm front position, where there is no well defined boundary layer;
- A frontal ageostrophic secondary circulation with the surface ageostrophic wind moving from the cold air to the warm, with upward motion in the warm air.

From the last two above items, it is clear that surface fluxes must be in the warm sector for them to directly feed the ascending air and warm the atmosphere. This is contrary to the study by Fleagle and Nuss (1985) of west coast, non-explosive storms, which placed the largest upward fluxes in the cold sector with small or negative surface fluxes in the warm sector. However, in Nuss's (1989) simulation of the effects of surface heat and moisture fluxes on cyclogenesis, rapid development was associated with upward surface moisture fluxes in the warm sector and boundary layer stability differences across the warm front that apparently enhanced frontal convergence. It is not known whether these processes occur in actual explosive cyclones.

Investigation into explosive cyclogenesis has been hindered by a lack of observations on the small scale. Most studies and their conclusions are based on synoptic scale anal-

ysis with limited observations. This thesis will attempt to resolve the role of surface heat and moisture fluxes and horizontally varying boundary layer structure by examining the details of the boundary layer structure of an explosive cyclone in the warm front region. More specifically, this thesis has the following objectives:

1. Map the detailed horizontal boundary layer structure of an open ocean explosive cyclone using one minute averaged aircraft data.
2. Describe the distribution of surface heat and moisture fluxes in relation to the warm front.
3. Describe the stability structure of the boundary layer across the warm front.
4. Examine the effect that the distribution of surface heat and moisture fluxes, and PBL stability structure, have on the frontogenesis and ageostrophic secondary circulation of the warm front.

II. DATA AND MODEL DESCRIPTION

The Experiment on Rapidly Intensifying Cyclones over the Atlantic (ERICA) was devised to "determine physical mechanisms and processes, and their critical spatial and temporal combinations, which can account for the winter time phenomenon of explosively developing over-ocean atmospheric storms." (Hadlock and Kreitzberg 1988). Conducted from 1 December 1988 to 1 March 1989, the area of interest was centered off the east coast of the United States in a climatologically favored region for explosive cylogenesis extending from 40°N to 47°N between 59°W and 69°W (Hadlock and Kreitzberg 1988). The ERICA field study encompassed six explosive cyclones with intensive observation periods (IOPs) of aproximately 36 hours covering the period of explosive development. This thesis examines a portion of the second intense observation period (IOP-2) from 0300 UTC to 0700 UTC 14 December, which was the initial stage of rapid cyclogenesis.

For IOP-2 a variety of data were obtained. The horizontal PBL structure was determined by a NOAA WP-3D which was tasked to document the PBL structure by flying a sawtoothed flight profile across the warm front. Vertical structure was to be measured by aircraft deployed dropwindsondes, of which only one provided good data. The aircraft data were supplemented by three drifting buoys from a field of fifty drifting buoys at 200 km spacing which measured mean sea-level pressure, air temperature, and sea-surface temperature (SST) on an hourly basis. Satellite SST measurements and standard ship observations were also available and used in this study.

The IOP-2 aircraft data which were as used to construct detailed horizontal analyses, consisted of 76 meteorlogical and flight parameters recorded at one-second intervals. The first step in processing the data for this thesis was to time average the data over 60-second intervals in order to reduce the data set to a more managable size and remove very small scale variablity that could not be resolved in the horizontal analysis. Care was taken not to average over any data gaps or around turns where wind data may be questionable. Horizontal homogenity was maintained by rejecting any measurements taken when the aircraft was climbing or descending at greater than 5 m s^{-1} or if the aircraft significantly deviated from the desired altitude of 350 m.

A Cressman analysis scheme was then employed to produce gridded data fields from these processed aircraft observations. The Cressman analysis was done over a 500 km

by 350 km grid with a 10 km grid spacing. This grid relative to the aircraft track is shown in Fig 1. Five analysis passes were made on the data using decreasing scan radii of 20.0, 15.0, 10.0, 7.0, and 3.0 km. This thesis treats the four-hour data acquisition effort as a 'snapshot' of the storm and no corrections for system translation were made. A correction for system translation would entail an assumption of quasi-steady state that was not justified given that the cylone deepened 12 mb over the four hours when data were taken. It is believed that the errors associated with any such correction may be comparable to analysis errors with no correction. While this assumption about the error, when no translation correction is made, may not be true in general, several factors minimize the errors in this case.

- The warm front was quasi-staionary during the flight and the cyclone moved eastward along the warm front. Consequently, structure to the east of the the low is not influenced by substantial translation of the primary feature and there is little blending of substantially different data, which gives relatively small errors. To the west of the low, the analysis consists of pre-cyclone and post-cyclone data and the error is larger due to this blending;
- The aircraft track moved to the east with the system so that the majority of the data are in the warm front region. In addition, the translation of the cyclone was relatively short compared to the data coverage to the east of the cyclone. This favors the analysis of the warm front which is the primary focus of this study.

Consequently, the analysis in the warm frontal region are believed to be representative of the structure even with some time averaging of this structure.

The data fields were then passed to the Brown-Liu marine planetary boundary layer model for calculation of surface winds and wind stress, and surface heat and moisture fluxes. This PBL model is a two-layer model with an Ekman Taylor layer over a logarithmic surface layer. The model calculates surface fluxes and winds given an upper boundary condition which can be the top of the PBL or within the Ekman layer. The flight level winds are taken as the winds within the Ekman layer from which surface winds are calculated. The air temperature field is required for thermal wind effects while the air-sea temperature difference from air and sea temperature fields is needed to calculate PBL stratification and surface fluxes (Brown and Liu 1982).

The Brown-Liu model requires surface air temperature and relative humidity to calculate the initial surface fluxes to determine the stability and iteratively solve for the surface fluxes. This required that the flight level data be extrapolated down to the surface. To make this extrapolation, a well mixed PBL with constant equivalent potential temperature (θ_e) and mixing ratio (q) was assumed. The temperature (T) can then be determined by the relationship

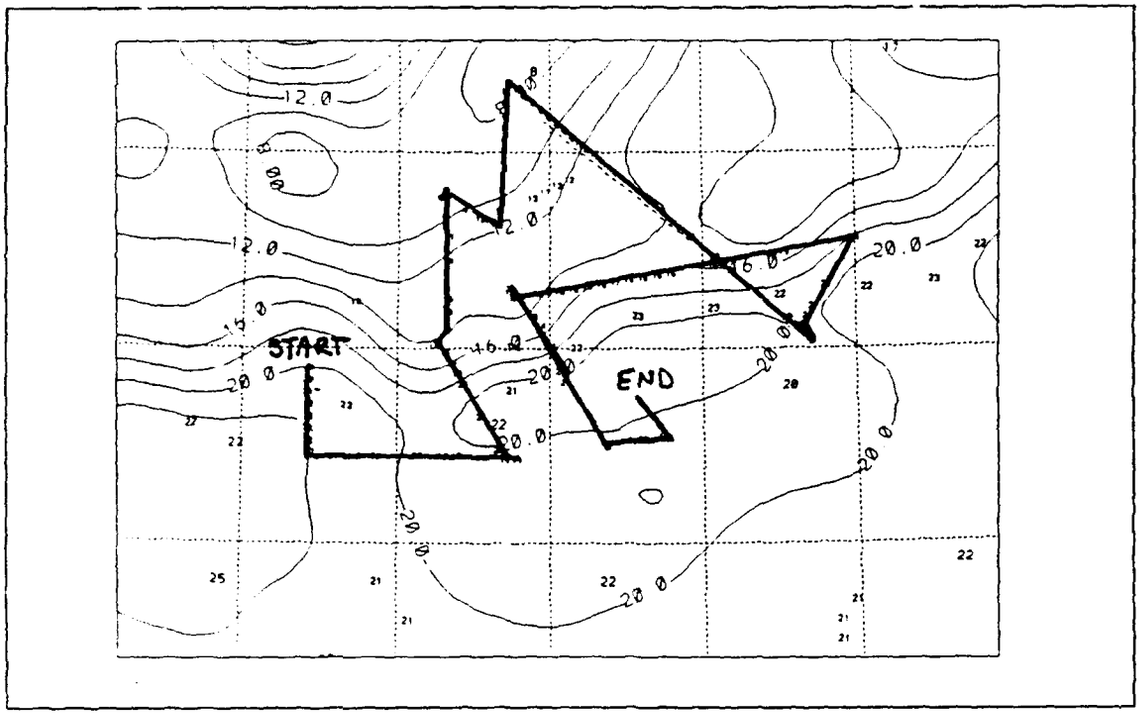

Figure 1. IOP-2 Aircraft track relative to analysis grid.

$$T = \theta_e \left(\frac{P}{1000} \right)^{.286} - \frac{L}{C_p} q \,,$$

where p is the pressure at flight altitude, L is the latent heat of vaporization, C_p is the specific heat at constant pressure, q is the mixing ratio, and θ_e is equivalent potential temperature measured at the aircraft. To determine relative humidity (R) at the surface, the saturation vapor pressure (e_s) was calculated using the derived surface temperature field and the following relationship between vapor pressure and temperature;

$$e_s = 6.1078 \times 10^{\frac{7.5 \times T - 273.16}{T - 35.86}} \,.$$

Saturated mixing ratio (q_s) was then calculated from the saturation vapor pressure and surface air pressure given by the following equation:

$$q_s = 0.622 \left(\frac{e_s}{p - e_s} \right) .$$

Finally, the relative humidity field was calculated using the aircraft mixing ratio (q) and the derived saturation mixing ratio (q_s) using the standard formulation for relative humidity;

$$R = \frac{q}{q_s} .$$

To determine surface fluxes,the model requires that the air-surface temperature and the air-surface humidity differences be calculated. The necessary SST field was created using multiple data sources in a Cressman analysis scheme. A first guess SST field was derived from a NESDIS Local-Scale Analysis Region 6 gridded SST field with a 14 km resolution. Because the Tiros-N series polar orbiting satellites only retrieve SST's under clear conditions, the age of the observations used in the analysis are variable. The particular analysis used was performed at 0107 UTC 14 December 1988, but the youngest satellite data are at least 12 hours old, and the majority of the observations were 132 hours old. The 14 km analysis was interpolated onto a 70 x 55 10 km grid centered on the 50 x 35 10 km grid used for the other data fields. To eliminate any boundary effects, the outer 10 grid points were discarded after the analysis was completed.

Three other data sources were used in the analysis: Radiometric temperatures from the aircraft, and sea-surface temperatures from ships and buoys. The aircraft's downward looking radiometer observations were then screened to eliminate erroneous data:

1. All readings from altitudes greater than 500 m were discarded (water vapor and or undetected clouds in the column below the aircraft can give a cold bias);
2. One-minute averages were discarded if any one second had
   a. a relative humidity greater than 88%, or
   b. a liquid water content greater than 0.3 g kg^{-1}, or
   c. a relative humidity greater than 82% and a liquid water content greater than 0.2 g kg^{-1}
3. Data were not discarded on the basis of aircraft turns or ascent descent rate.

Because the satellite observations were largely 132 hours old and also because the ship and buoy data outside the aircraft flight path were quite sparse, ship and buoy data dating back to 0000 UTC 9 December were examined. Ship data were included only if they were within approximately 3° of the satellite field or were strongly supported by independent aircraft or buoy data. Older data and especially old data near strong gradi-

ents were more critically examined. Most all of the buoy data were included, except in cases where redundant older data were discarded in favor of collocated younger data.

The final analysis was performed using a Cressman scheme with a limit of 8 degrees on the difference from the first guess imposed as a final check on the data quality. Scan radii of 10.0, 5.0, 2.5, 1.0, and 0.5 km were used on five successive passes. Given the combination of sparse and clustered observations, these scans most closely replicated a hand analysis.

III. IOP-2 SYNOPTIC SUMMARY

As discussed in Chalfant (1989), IOP-2 is characterized by the development of several cyclones associated with the advance of several short wave troughs in rapid succession. The first cyclone developed well to the south and underwent a brief period of moderate deepening before it weakened rapidly. While the first cyclone was beginning to weaken, a much more significant cyclone had begun to develop to the southwest just off the North Carolina/Virginia coast. This second cyclone underwent very rapid cyclogenesis to become the dominant feature. The 0600 UTC 13 December 1988 (from here on, date and time will be given as date time UTC, e.g. 13 0600 UTC) mean sea-level pressure and isotherm analysis from Sanders (1989) show the low-level structure associated with the first cyclone (Fig. 2). The cold advection evident in Fig. 2 is associated with the 992 mb low to the southeast of Newfoundland at 43°N, 47°W and the 1028 mb high off the New England coast at 48°N, 65°W.

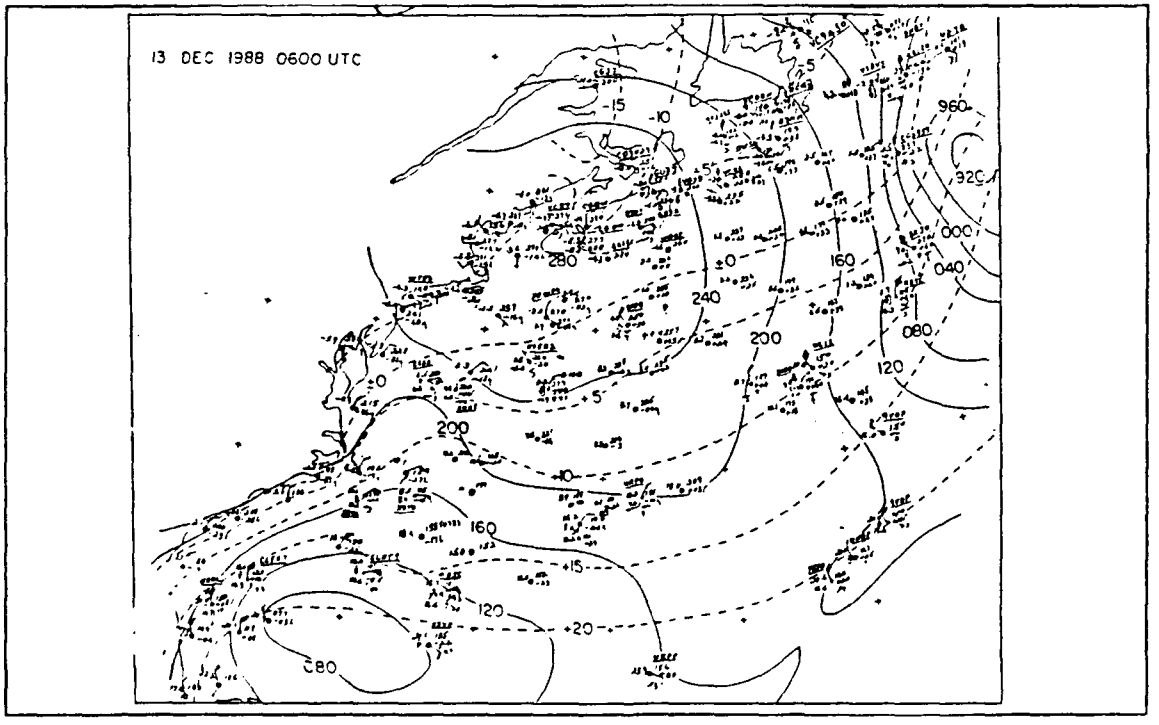

Figure 2. IOP-2 13/0600 UTC surface analysis: Sea-level pressure (solid) in tenths of mb where the leading 9 or 10 has been dropped and surface temperature (dashed) in °C. (Sanders 1989).

By 13/1800 UTC, both surface cyclones are evident as two distinct low centers embedded in a large area of cyclonic circulation (Fig. 3) just off the East Coast. The northern cyclone, with a central pressure of 1004 mb is located in a region of very little thermal gradient and very weak warm thermal advection east of the low (Fig. 3) but is apparently near the north wall of the Gulf Stream where a substantial surface temperature gradient exists. Differencing the isotherm analysis at 13/06 UTC and 13/18 UTC reveals a region of greater than 5° C warming over 12 hours to the north and east of the cyclone. The maximum warming occurs just east of the northern low pressure center at about 37.5°N, 68°W which is near the location of the Gulf Stream. Although this analysis is only approximate, this rapid warming in a region of weak thermal advection and near the the maximum SST gradient is certainly suggestive of warming from the surface fluxes associated with the Gulf Stream. Substantial upper-level vorticity advection is found over this northern cyclone in synoptic scale 500 mb analyses (not shown). Hence, there is ample support for cyclogenesis to occur in this region.

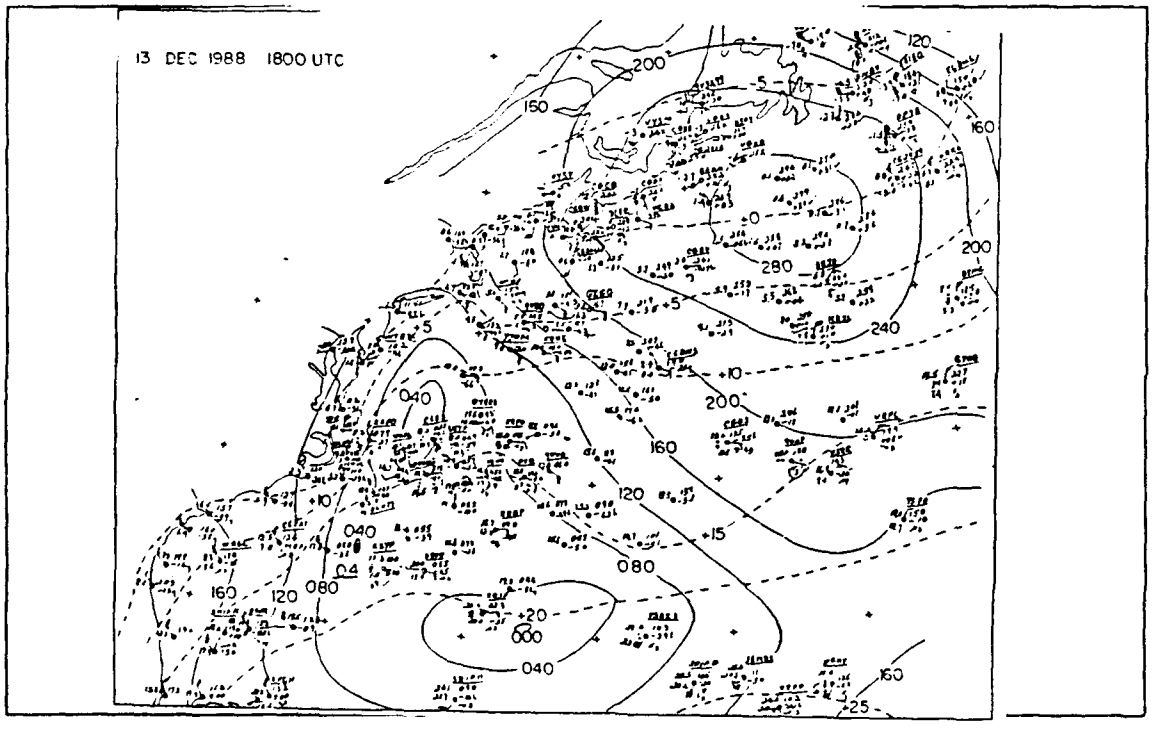

Figure 3. IOP-2 13/1800 UTC surface analysis: Same as figure 2 (Sanders 1989).

At 14/0000 UTC, this northern low at 37°N, 70°W with a central pressure of 996 mb, began explosive development. Examining the 14/0000 UTC mean sea-level pressure and isotherm analysis (Fig. 4), warm advection has increased at the surface just east of this cyclone. However, the largest surface warming is found to the northeast (40°N, 64°W) where little warm advection is found. Extremely rapid warming of 5° C in 6 hours in the region to the northeast is highly suggestive of heating due to surface fluxes. A more substantial thermal gradient develops as the cyclone intensifies which may be due in part to surface warming by the heat flux. The position of the low center coincides with the northern boundary of the Gulf Stream as indicated by satellite SST analysis. This relationship between the surface low center and the Gulf Stream was maintained during most of the explosive development which yielded a cyclone track along the Gulf Stream (Fig. 5). It is possible that such movement would enhance cyclogenesis as the increased surface fluxes over the Gulf Stream increases the frontogentical forcing of the ageostrophic secondary circulation associated with the warm front. Detailed analysis using the aircraft data will explore this question in the next section.

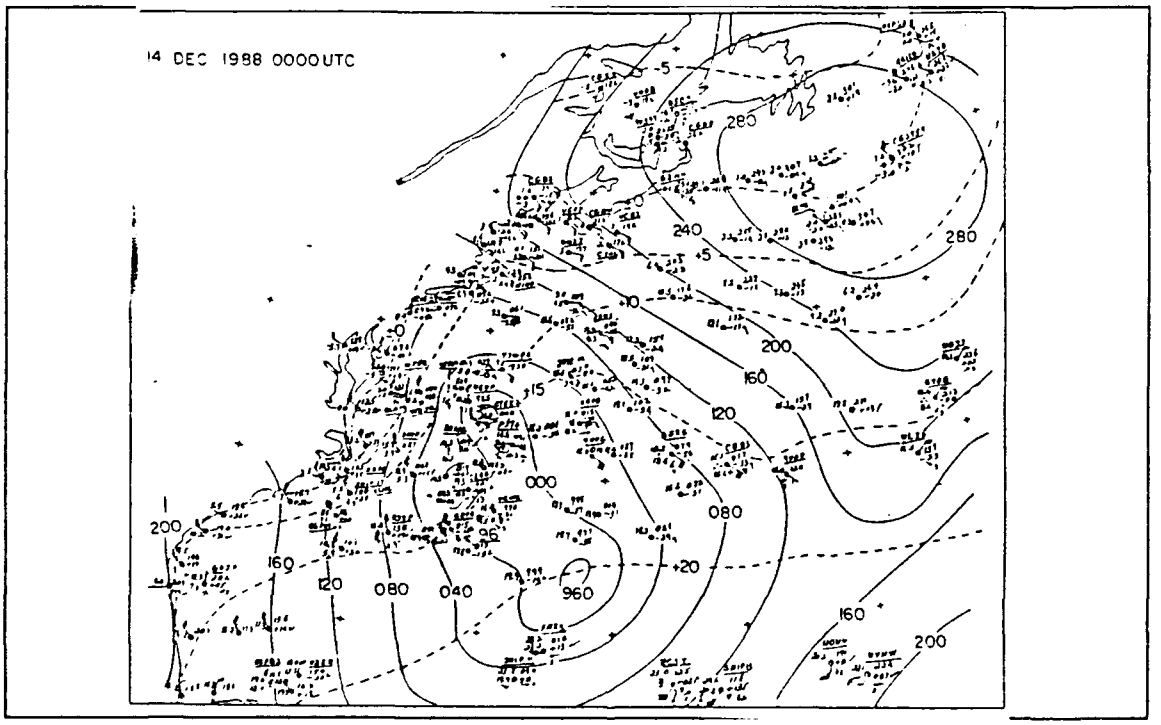

Figure 4. IOP-2 14/0000 UTC surface analysis: Same as figure 2 (Sanders 1989).

During the next 12 hours this cyclone deepened 30 mb to become a 968 mb low at 14/1200 UTC as shown in Fig. 6. The first cyclone to the south stopped developing and was rapidly absorbed into this much more intense northern cyclone. The low-level structure at this time is typical of many mature cyclones with well defined warm and cold fronts and the beginning of the occlusion process. The cyclone fills during subsequent time periods.

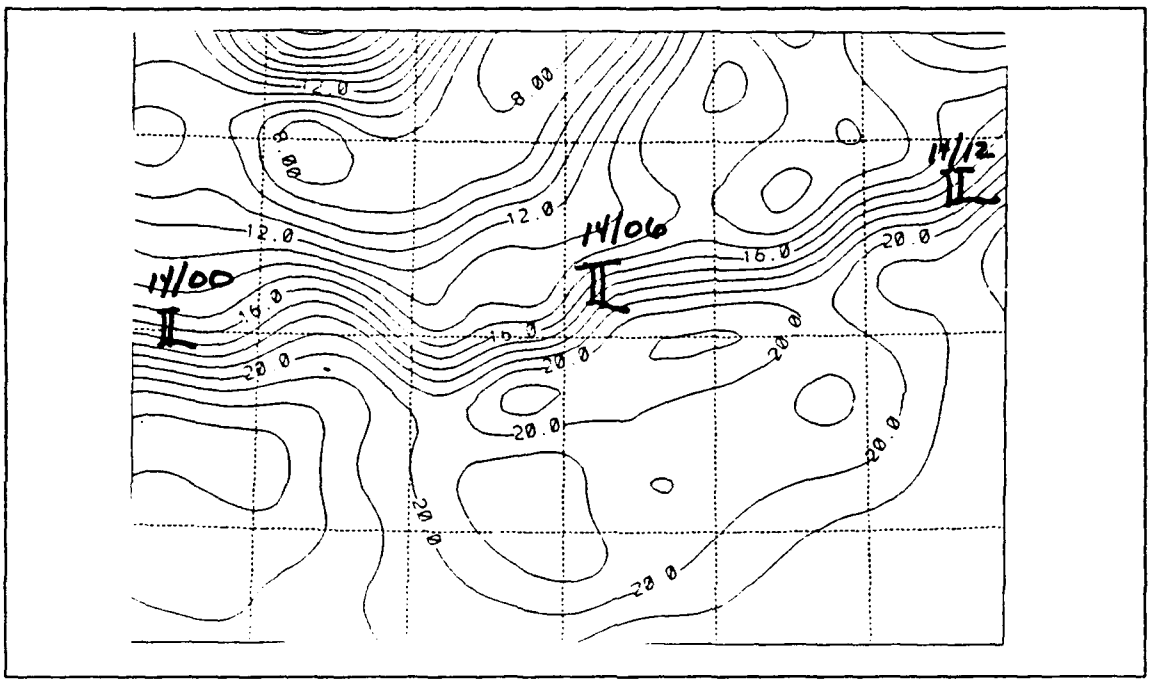

Figure 5. IOP-2 Cyclone track: SST isotherms in °C.

To summarize, IOP-2 was a multiple low event triggered by the offshore movement of two upper air short wave troughs 12 hours apart. A surface low developed east of Florida in response to the first trough. The second upper air trough triggered the formation of two new lows in a surface trough that extended north of the initial system. The northernmost system developed explosively while moving along the northern boundary of the Gulf Stream in a region that had experienced rapid warming over the preceeding 18 hours, while the other two systems weakened and were assimilated into this major cyclone. Crude warming charts constructed using the temperature change over successive isotherm analyses suggest that surface fluxes along the Gulf Stream potentially contributed to this extraordinary cyclone and will be explored in detail in the following section.

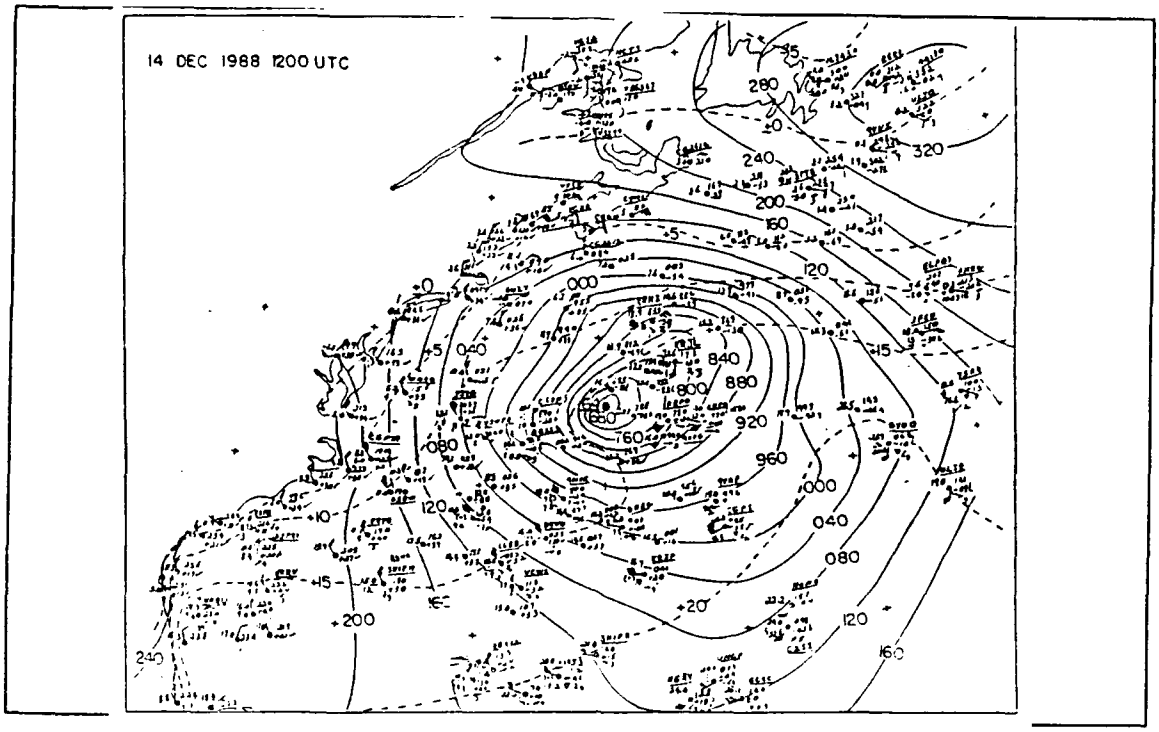

Figure 6. IOP-2 14/1200 UTC surface analysis: Same as figure 2 (Sanders 1989).

IV. BOUNDARY LAYER ANALYSIS

From the synoptic examination in the previous section, the pattern which emerges is that the cold advection associated with the preceeding cyclone produced large surface heat and moisture fluxes that feed the developing cyclone in IOP-2. The fluxes may have contributed to warm frontogenesis along the Gulf Stream where the cyclone tracked. The aim of this section is to examine in detail the surface flux distribution and boundary layer structure around the warm front during the initial phase of explosive development. As described in section II, the aircraft data were analyzed on a grid for this analysis.

The detailed surface structure at around 14 0600 UTC is shown in Fig. 7. The surface low and frontal positions are taken from a separate hand analysis of the aircraft observations of winds and pressure. The horizontal surface air temperature distribution along the warm front shows a 3°C gradient from 18°to 21°C approximately coincident with the SST gradient. Also apparent is the cold front extending north south along 66.5°W. The gridded thermal gradient is not exactly correspondent to the frontal analysis due to the data blending resulting from system translation to the east and smoothing inherent in the objective analysis method. There is, however, a high degree of confidence in the computed distribution about the warm front due to lack of blending as previously detailed in Section II. With this in mind, analysis will concentrate on the warm frontal and warm sector structure of IOP-2.

The surface heat flux distribution around the warm front (Fig. 8) shows downward fluxes to the north of the front and upward fluxes to the south. The magnitude of the downward fluxes to the north of the warm front are generally small (less than -50 W m^{-2}) with more significant upward fluxes (+ 100 Wm^{-2}) to the south of the front. The small magnitude of the fluxes north of the front indicates that the air over the cold water is in near equilbrium with the sea-surface temperature. The maximum heating essentially coincides with the SST gradient, which suggests the advection of cold air over the Gulf Stream. The increase in fluxes towards the east suggests that the air is being modified as it flows in from the east. This flux distribution is opposite to the distribution observed by Petersson et. al. (1962) and Fleagle and Nuss (1985) where cooling occurred in the warm air and warming occurred in the cold air. This distribution of heating results in warm frontogenesis to increase the baroclinicity of the system, which is similar to the

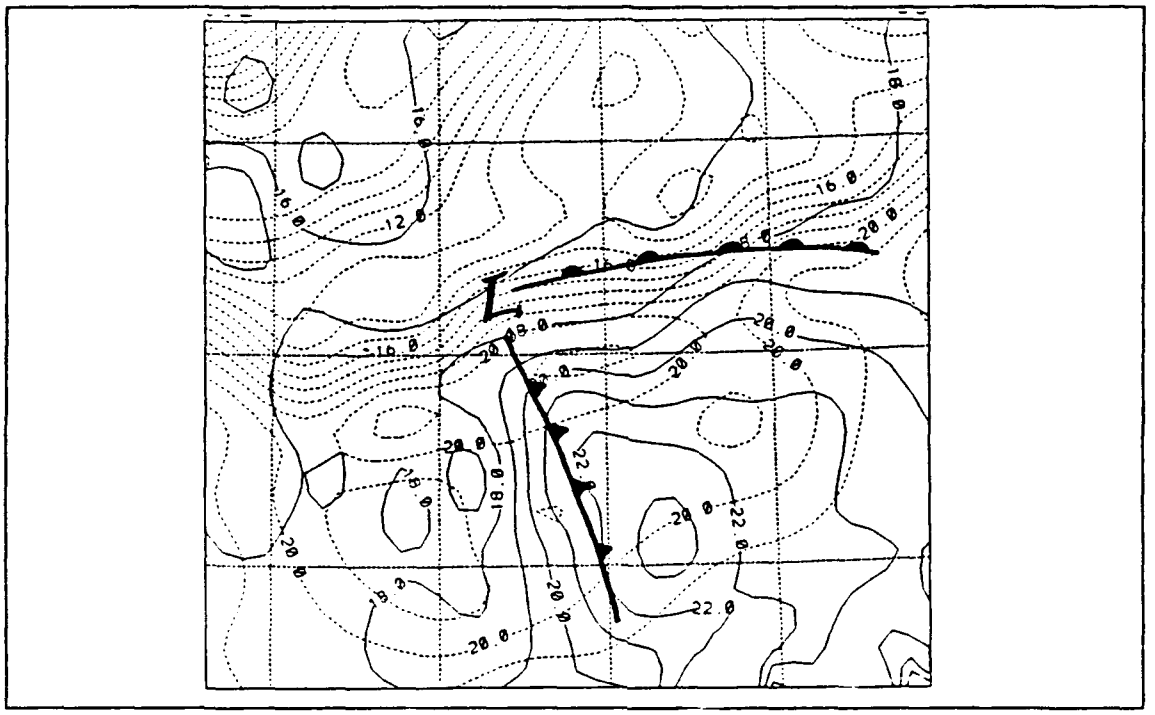

Figure 7. IOP-2 surface structure: Surface temperature (solid) and SST (dashed) in °C analyzed from aircraft data. Latitude and longitude in one degree *increments with a center* latitude and longitude of 38°N and 66°W.

flux influence on the coastal frontogenesis in the Presidents' Day storm and is suggestive of some arctic ice edge polar lows.

The moisture fluxes (Fig. 9) are considerably stronger than the heat flux, with 500 Wm^{-2} upward fluxes south of the warm front and relatively weaker upward fluxes to the north. The magnitude of the fluxes in the cyclone's warm sector are very large and approach values recorded in cold air outbreak studies. However, these large moisture fluxes are occurring in the warm sector of a developing cyclone where they will feed the cloud and precipitation region of the cyclone. As with the heat flux, the SST and moisture flux gradients are essentially coincident, which emphasizes the role of the Gulf Stream boundary in creating the flux distribution. In addition, the moisture flux tends to increase towards the east, which suggests that the easterly winds in this region are bringing in relatively dry air that is modified by the moisture flux.

The fact that these strong moisture fluxes persisted throughout the initial phase of explosive development implies a continuous supply of cold, dry air over the warm water.

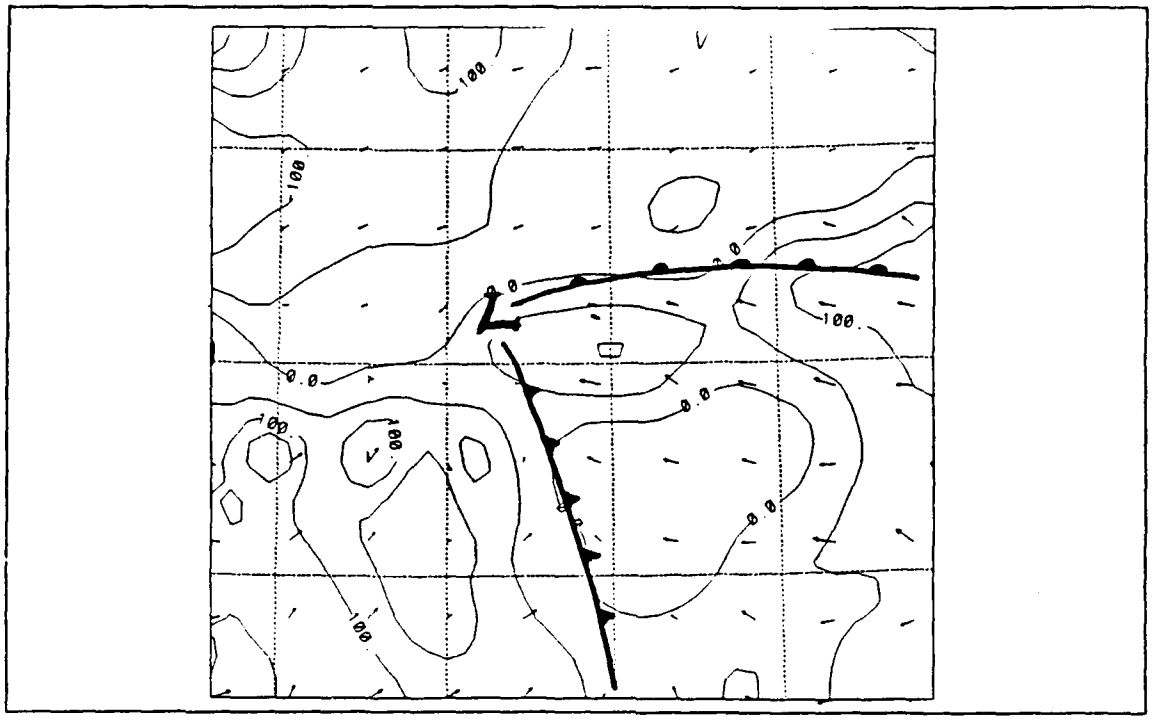

Figure 8. IOP-2 surface sensible heat flux: Sensible heat flux in W m^{-2}. Grid as in Fig. 7.

Such a situation is not consistant with the expected warm advection from the south predicted by traditional mid-latitude cyclone theory. Examination of the surface wind analysis (Fig. 10) reveals strong easterly flow with a wind maximum of 26 m s^{-1} located south of the warm front. These strong easterly winds are consistant with the frontogenesis mechanism proposed by Grotjahn and Wang (1989) whereby air from the cold sector of a preceding cyclone is drawn into the warm sector of a following cyclone. The 13 0600 UTC synoptic analysis (Fig. 2) shows such a preceding cyclone to the northeast of the incipient explosive cyclone. A study of the boundary layer over a larger region that includes the tracing of air parcel trajectories would be required to confirm that air parcels move from the cold sector of the previous low into this region of the warm front. While this is beyond the scope of this study, the wind flow near the front in the small scale analyses do support this interpretation.

As discussed above, the moisture fluxes are advantageously placed to feed the warm frontal updraft region and thus enhance latent heat release. As suggested by Davis and Emanual (1989), surface heat and moisture fluxes may act to destabilize moist symmet-

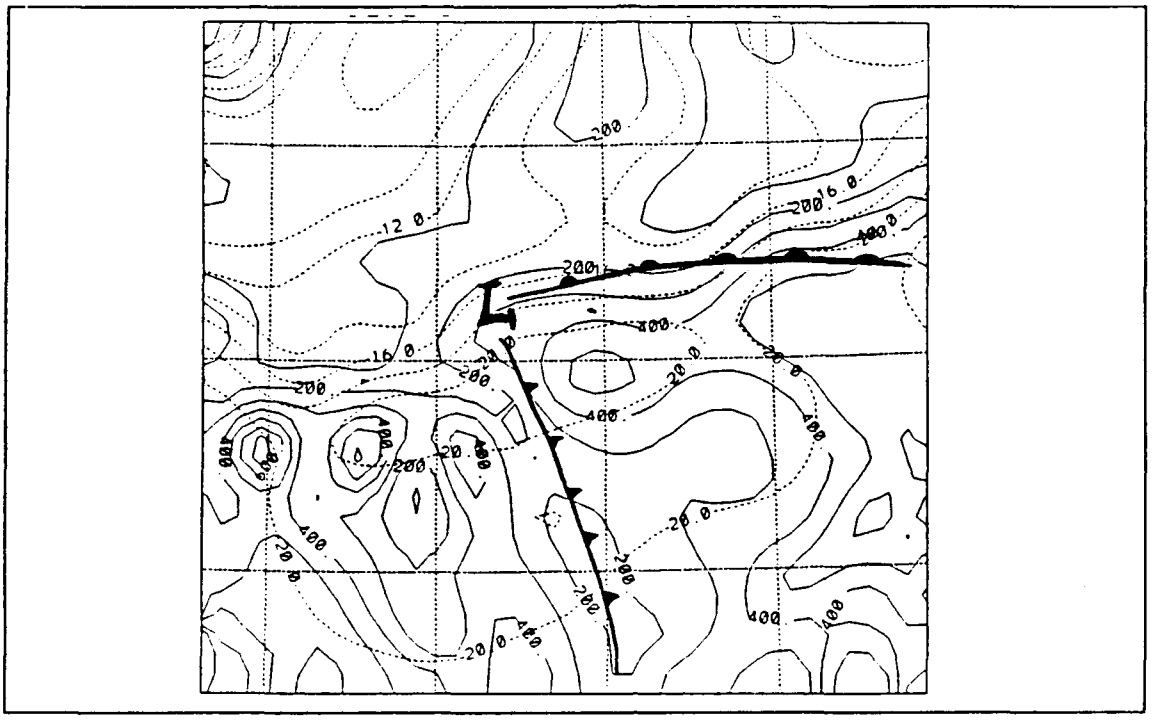

Figure 9. IOP-2 surface latent heat flux: Latent heat flux (solid) in W m^{-2}. SST (dashed) in °C. Grid as in Fig 7.

rically neutral regions and produce deep slantwise convection in the warm frontal region. While no analysis of the stability was done, vertical or slantwise, both satellite and radar images (not shown) show strong convection along the warm front with radar returns on the order of 50 dbz being recorded. The warming and moistening by the fluxes in this region may contribute to the convective instability and clearly supply moisture to the clouds. A more detailed analysis of the deeper structure is required to quantify the contribution of these fluxes to the convection.

Nuss (1989) highlighted the frontogenetical role of enhanced horizontally varying momentum transfer to the sea surface due to the destabilizing effects of surface fluxes in the boundary layer. While conclusive dropsonde data is not available for the cyclone's warm sector, some idea of boundary layer stability can be inferred from comparing flight level winds and surface winds. South of the warm front, surface wind speeds are equal to flight level winds. This indicates a deep, well mixed boundary layer with flight level winds being mixed down to the surface, which agrees with the upward heat fluxes in this region. In contrast, surface winds north of the warm front are only one half the strength

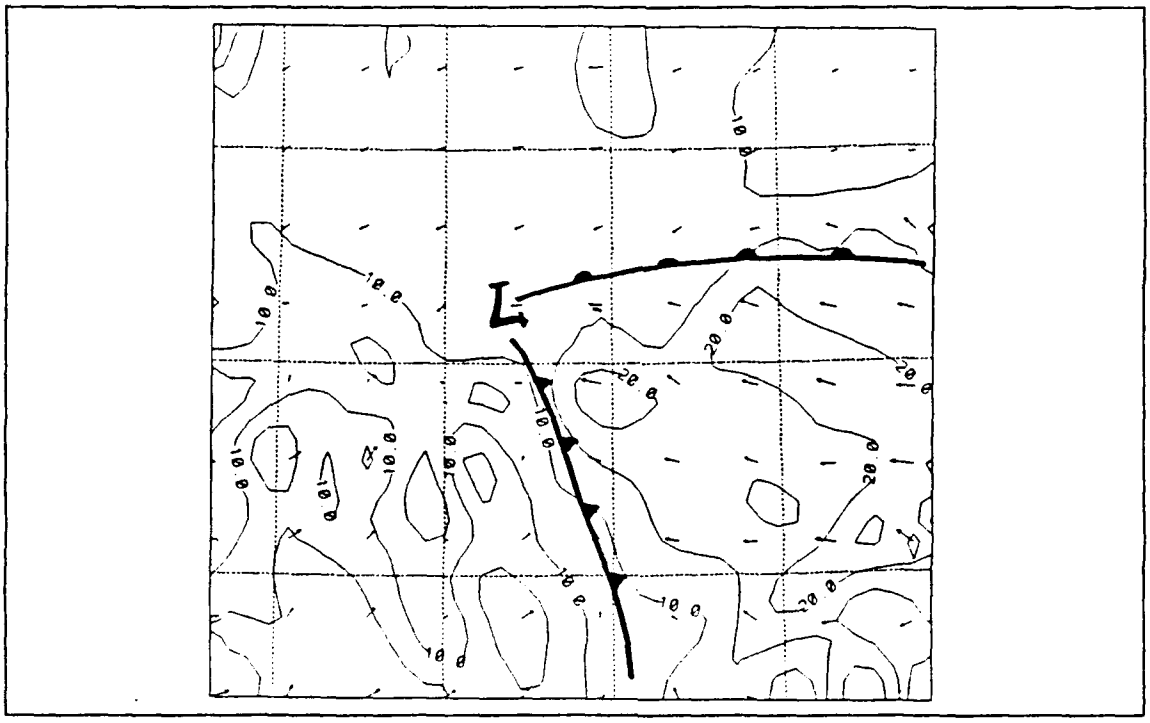

Figure 10. IOP-2 surface winds: Isotachs in 5 m s^{-1} intervals. Grid as in Fig 7.

of flight level winds, indicating a more stable boundary layer, also in agreement with the downward fluxes in this region. The less stable boundary layer in the cyclone's warm sector would enhance the transfer of momentum to the surface as suggested by Nuss (1989) but this increased momentum transfer is on the opposite side of the warm front as found in the numerical simulations. However, the effect is similar in that the resultant surface winds are more convergent than those at the flight level of the aircraft. This frictional convergence is frontogenetical which is evident from the observed structure.

The boundary layer structure that emerges from this analysis near the warm front differs from that described in west coast cyclones by Fleagle et al. (1988). The unstable, well-mixed boundary layer occurs in the warm sector and is apparently maintained by the easterly flow of dry, cold air. A more stable boundary layer occurs north of the warm front where the air has apparently reached near equilibrium with the sea surface. This structure favors frontogenesis through direct diabatic heating from the sea surface and through its influence on the horizontally varying friction.

To further highlight the potential impact of this boundary layer structure on the dynamics of the cyclone, a qualitative examination of the Q-vector form of the omega

equation, as given by Hoskins et al. (1978) was made. As the Q-vectors will be used descriptively and no vectors are actually calcilated, only a brief discussion of Q-vectors will be provided. A complete derivation of the Q-vector form of the omega equation can be found in Appendix A. The Q-vector form of the omega equation is written as

$$\left(\nabla^2 + \frac{f_0^2}{\sigma}\frac{\partial^2}{\partial p^2}\right)\omega = -2\nabla \cdot \vec{\mathbf{Q}},$$

where $\sigma \equiv -f_0\gamma\frac{\partial\theta}{\partial p}$ is the static stability parameter and

$$\vec{\mathbf{Q}} = (Q_1, Q_2) = \left(-\gamma\frac{\partial \vec{V}_g}{\partial x}\cdot\nabla\theta, -\gamma\frac{\partial \vec{V}_g}{\partial y}\cdot\nabla\theta\right).$$

This form of the omega equation ignores the effects of diabatic processes in forcing vertical motion. If the atmosphere is saturated, then one can directly include the effects of latent heat release on the vertical motion by considering the forcing in terms of moist baroclinic dynamics. Therefore, a moist Q-vector can be defined by assuming that in a saturated atmosphere θ_e is equivalent to θ. Substituting θ_e for θ in the Q-vector omega equation results in

$$\vec{\mathbf{Q}} = (Q_1, Q_2) = \left(-\gamma\frac{\partial \vec{V}_g}{\partial x}\cdot\nabla\theta_e, -\gamma\frac{\partial \vec{V}_g}{\partial y}\cdot\nabla\theta_e\right).$$

which gives the geostrophic frontogentical forcing of vertical motion in a saturated enviroment. A more complete description of the moist frontogenesis can be obtained by examining the two dimensional frontogenesis equation. The moist frontogenesis equation is

$$\frac{\partial}{\partial t}\left(\frac{\partial\theta_e}{\partial y}\right) = -\frac{\partial}{\partial y}\left(\frac{d\theta_e}{dt}\right) - \frac{\partial u_g}{\partial y}\frac{\partial\theta_e}{\partial x} - \frac{\partial v_g}{\partial y}\frac{\partial\theta_e}{\partial y} - \frac{\partial\omega}{\partial y}\frac{\partial\theta_e}{\partial p}.$$

The first term represents non-conservative moist processes and is zero except at the sea surface where surface heat and moisture fluxes alter θ_e due to interaction with the boundary. The second and third terms represent the horizontal geostrophic deformation of the θ_e gradient, which is the moist Q-vector forcing. Although the geostrophic forcing is not known in this case, the total wind and θ_e distribution suggest moist frontogentical forcing by the horizontal deformation (Fig. 10). In the warm sector south of the warm

front, large ($\simeq$500 W m^{-2}) upward surface moisture fluxes and upward surface heat fluxes act to increase surface θ_e and strengthen frontogentical forcing of the warm front. This warming and moistening of the warm sector also destabilizes the boundary layer in the cyclone's warm sector, which apparently results in enhanced convection along the warm front. This enhanced vertical motion would then strengthen the geostrophic deformation as indicated by the Q-vector omega equation, which potentially enhances the cyclogenesis. While this analysis is rather speculative, it does suggest the possible dynamical processes by which the surface fluxes enhance cyclogenesis in this case. It remains to be shown through a more quantitative analysis whether the surface fluxes contribute as significantly as suggested by this qualitative analysis.

V. CONCLUSIONS AND RECOMMENDATIONS.

The detailed boundary layer analysis of IOP-2 has shown that the distribution of surface fluxes about the warm front in an explosive cyclone provides favorable frontogentical forcing to increase cyclogenesis. Specifically, this study has shown:

1. The horizontal boundary layer structure of the cyclone during its explosive phase, when accurately mapped on a small scale using aircraft data, has a boundary layer structure that differs from that found in typical cyclones.
2. Heat fluxes about the warm front were relatively small due to air and sea surface temperatures being in near equilibrium. In contrast, large upward moisture fluxes were present south of the warm front with weaker fluxes to the north of the front.
3. Boundary layer stratification was stable to the north of the warm front and unstable to the south of the warm front. This resulted in different momentum fluxes on either side of the front to produce convergence in the surface winds.
4. The surface heat and moisture flux distribution as well as the wind field are favorable for moist frontogenesis along the SST gradient. Given nearly saturated conditions, this enhanced surface frontogenesis would contribute significantly to the cyclogenesis.

While the analysis points to a potentially large role for surface fluxes in explosive cyclogenesis, the limitations inherent in this single case study suggest the following recommendations for further research:

1. This analysis of the PBL in a limited region should be extended to a larger domain and include a trajectory analysis.
2. A complete 3-D analysis should be done to examine the dynamics that are driving the ageostrophic circulation.
3. The time evolution of the cyclone and PBL structure should be determined.
4. Extend this analysis to ERICA IOPs with intermittent explosive development. A comparison of the surface flux distribution and magnitude during explosive and non-explosive phases would highlight any possible differences in the role of the boundary layer processes.

APPENDIX A. Q-VECTOR DERIVATION

Derivation of the Q-vector form of the omega equation begins with the quasi-geostrophic momentum, thermodynamic and continuity equations:

$$\left(\frac{\hat{c}}{\hat{c}t} + \vec{V}_g \cdot \nabla\right) U_g = f_o V_{ag} + \frac{\partial f}{\hat{c}y} V_g + F_x ,$$

$$\left(\frac{\hat{c}}{\hat{c}t} + \vec{V}_g \cdot \nabla\right) V_g = -f_o U_{ag} + F_y ,$$

$$\left(\frac{\hat{c}}{\hat{c}t} + \vec{V}_g \cdot \nabla\right)\theta + \omega \frac{\hat{c}\theta}{\hat{c}p} = Q ,$$

$$\frac{\hat{c}u_{ag}}{\hat{c}x} + \frac{\hat{c}v_{ag}}{\hat{c}y} + \frac{\hat{c}w}{\hat{c}p} = 0 \text{ and}$$

$$\frac{\hat{c}u_g}{\hat{c}x} + \frac{\hat{c}v_{ag}}{\hat{c}y} = 0 .$$

For the Q-vector derivation the following assumptions are then made:

1. f plane $\frac{\hat{c}f}{\hat{c}y} = 0$,
2. frictionless $F_x = F_y = 0$,
3. adiabatic $\dot{Q} = 0$ and
4. constant static stability $\frac{\hat{c}\theta}{\hat{c}p} = constant.$

Momentum equations are then differentiated by $\frac{\hat{c}}{\hat{c}p}$ and the thermodynamic equation by $\frac{\hat{c}}{\hat{c}x}$ or $\frac{\hat{c}}{\hat{c}y}$. For the x component equation:

$$\frac{\hat{c}}{\hat{c}p}\left[\left(\frac{\hat{c}}{\hat{c}t} + \vec{V}_g \cdot \nabla\right) U_g - f_o V_{ag} = 0\right] \text{ and} \tag{1}$$

$$\gamma \frac{\hat{c}}{\hat{c}y}\left[\left(\frac{\hat{c}}{\hat{c}t} + \vec{V}_g \cdot \nabla\right)\theta + \omega \frac{\hat{c}\theta}{\hat{c}p} = 0\right] \tag{2}$$

Equation (1) becomes

$$\left(\frac{\partial}{\partial t} + \vec{V}_g \cdot \nabla\right)\frac{\partial u_g}{\partial p} + \frac{\partial \vec{V}_g}{\partial p} \cdot \nabla U_g - f_o \frac{\partial v_{ag}}{\partial p} = 0 \tag{3}$$

and equation (2) becomes

$$\left(\frac{\partial}{\partial t} + \vec{V}_g \cdot \nabla\right)\gamma \frac{\partial \theta}{\partial y} + \gamma \frac{\partial \vec{V}_g}{\partial y} \cdot \nabla\theta + \gamma \frac{\partial \omega}{\partial y}\frac{\partial \theta}{\partial p} = 0 . \tag{4}$$

Expanding the second term of equation (3),

$$\frac{\partial \vec{V}_g}{\partial p} \cdot \nabla U_g = \frac{\partial u_g}{\partial p}\frac{\partial u_g}{\partial x} + \frac{\partial v_g}{\partial p}\frac{\partial u_g}{\partial y} - \frac{\partial u_g}{\partial p}\left(\frac{\partial u_g}{\partial x} + \frac{\partial v_g}{\partial y}\right), \tag{5}$$

and by using the thermal wind relationships

$$\frac{\partial u_g}{\partial p} = \gamma \frac{\partial \theta}{\partial y} \quad ; \quad \frac{\partial v_g}{\partial p} = -\gamma \frac{\partial \theta}{\partial y}$$

and the fact that the horizontal divergence of the geostrophic wind is zero, (5) reduces to:

$$\frac{\partial \vec{V}_g}{\partial p} \cdot \nabla U_= - \gamma \frac{\partial \vec{V}_g}{\partial y} \cdot \nabla\theta \equiv Q_2 .$$

This term will be defined as Q_2 and is identical to, but of opposite sign to, the second term of (4). (3) and (4) can then be written as:

$$\left(\frac{\partial}{\partial t} + \vec{V}_g \cdot \nabla\right)\frac{\partial u_g}{\partial p} + Q_2 - f_o \frac{\partial v_{ag}}{\partial p} = 0 \text{ and} \tag{6}$$

$$\left(\frac{\partial}{\partial t} + \vec{V}_g \cdot \nabla\right)\gamma \frac{\partial \theta}{\partial y} - Q_2 + \gamma \frac{\partial \omega}{\partial y}\frac{\partial \theta}{\partial p} = 0 . \tag{7}$$

Since the first term of (6) and (7) are equal through the thermal wind equation, subtracting (7) from (6) results in

$$-f_0 \frac{\partial v_{ag}}{\partial p} - \gamma \frac{\partial \theta}{\partial p}\frac{\partial \omega}{\partial y} = -2Q_2 . \tag{8}$$

In quasi-geostrophic theory, geostrophic motion tends to destroy thermal wind balance which ageostrophic motion acts to restore. From (8) it can be seen that Q_2 represents a restoring force on geostrophic balance through differential ageostrophic horizontal motion acting on horizontal winds and differential vertical motion acting on the horizontal temperature gradient.

A completely analogous derivation for the y component produces

$$-f_0 \frac{\partial u_{ag}}{\partial p} - \gamma \frac{\partial \theta}{\partial p} \frac{\partial \omega}{\partial x} = -2Q_1 \text{ and} \tag{9}$$

$$Q_1 \equiv -\gamma \frac{\partial \vec{V}_g}{\partial x} \cdot \nabla\theta .$$

To obtain the omega equation, we differentiate (8) by $\frac{\partial}{\partial y}$ and (9) by $\frac{\partial}{\partial x}$ and add the two together:

$$-f_0 \frac{\partial^2 u_{ag}}{\partial p \partial x} - \gamma \frac{\partial \theta}{\partial p} \frac{\partial^2 \omega}{\partial x^2} = -2 \frac{\partial Q_1}{\partial x} \text{ and}$$

$$-f_0 \frac{\partial^2 v_{ag}}{\partial p \partial y} - \gamma \frac{\partial \theta}{\partial p} \frac{\partial^2 \omega}{\partial y^2} = -2 \frac{\partial Q_2}{\partial y} .$$

Adding yields:

$$-\frac{f_0}{\partial p}\left(\frac{\partial u_{ag}}{\partial x} + \frac{\partial v_{ag}}{\partial y}\right) - \gamma \frac{\partial \theta}{\partial p}\left(\frac{\partial^2 \omega}{\partial x^2} + \frac{\partial^2 \omega}{\partial y^2}\right) = -2\left(\frac{\partial Q_1}{\partial x} + \frac{\partial Q_2}{\partial y}\right) \tag{10}$$

Continuity is then used to obtain:

$$f_0 \frac{\partial^2 \omega}{\partial p_2} - \gamma \frac{\partial \theta}{\partial p} \nabla^2 \omega = -2\nabla \cdot \vec{\mathbf{Q}} .$$

where

$$\vec{\mathbf{Q}} = (Q_1 , Q_2) = \left(-\gamma \frac{\partial \vec{V}_g}{\partial x} \cdot \nabla\theta , -\gamma \frac{\partial \vec{V}_g}{\partial y} \cdot \nabla\theta\right) .$$

Further simplification results in

$$(\nabla^2 + \frac{f_0^2}{\sigma}\frac{\partial^2}{\partial p^2})\omega = -2\nabla \cdot \bar{\mathbf{Q}},$$

where $\sigma \equiv -f_0^2 \frac{\partial \theta}{\partial p}$ is the static stability parameter.

LIST OF REFERENCES

Bosart, L. F., and S. C. Lin, 1984: A diagonistic analysis of the Presidents' Day storm of February 1979. *Mon. Wea. Rev.*, **112**, 2148-2177.

Boyle, J. S. and L. F. Bosart, 1986: Cyclone-anticyclone couplets over North America. Part II: analysis of a major cyclone event over the eastern United States. *Mon. Wea. Rev.*, **114**, 2432-2465.

Brown, R. A. and W. T. Liu, 1982: An operational large-scale marine planetary boundary layer model, *J. Appl. Meteor.*, **21**, 261-269.

Chalfant, A., 1989: Dynamics of an ERICA cyclone, Masters' thesis, Naval Postgraduate School, Monterey, CA, 55pp.

Davis, C. A. and K. A. Emanuel, 1988: Observational evidence for the influence of surface heat fluxes on rapid maritime cyclogenesis, *Mon. Wea. Rev.*, **116**, 2649-2659.

Fleagle, R. G. and W. A. Nuss, 1985: The distribution of surface fluxes and boundary layer divergence in midlatitude ocean storms. *J. Atmos. Sci.*, **42**, 784-799.

-----, N. A. Bond, and W. A. Nuss, 1988: Atmosphere-ocean interaction in mid-latitude storms. *Meteorol. Atmos. Phys.*, **38**, 50-63.

Grotjahn, R. and C. H. Wang, 1989: On the source of air modified by ocean surface fluxes to enhance frontal cyclone development. *Ocean-Air Interactions*, **1**, 257-288.

Hadlock, R. and C. W. Kreitzberg, 1988: The experiment on rapidly intensifying cyclones over the Atlantic (ERICA) field study: Objectives and plans. *Bull. Amer. Meteor. Soc.*, **69**, 1309-1320.

Hoskins, B. J., I. Draghici, and H. C. Davis, 1978: A new look at the ω-equation. *Quart. J. R. Met. Soc.*, **104**, 31-38.

Kuo, Y. H. and R. J. Reed, 1988: Numerical simulation of an explosively deepening cyclone in the eastern Pacific. *Mon. Wea. Rev.*, **116**, 2081-2105.

Nuss, W. A., 1989: Air-sea interaction influences on the structure and intensification of an idealized marine cyclone. *Mon. Wea. Rev.*, **117**, 351-369.

Petterson, S., D. L. Bradbury and K. Pedersen, 1962: The Norwegian cyclone models in relation to heat and cold sources. *Geofys. Publ.*, **24**, 243-280.

Sanders, F., 1989: ERICA surface analysis. Available from ERICA data center, Drexel Univ., Philadelphia PA.

-----, and J. R. Gyakum, 1980: Synoptic-dynamic climatology of the "bomb". *Mon. Wea. Rev.*, **108**, 1589-1606.

Uccellini, L. W., P. J. Kocin, R. A. Peterson, C. W. Wash, and K. F. Brill, 1984: The Presidents' Day cyclone of 18-19 February 1979: Synoptic overview and analysis of the subtropical jet streak influencing the pre-cyclogenetic period. *Mon. Wea. Rev.*, **112**, 31-55.

-----, R. A. Peterson, K. F. Brill, P. J. Kocin, and J. J. Toccillo, 1987: Synergistic interaction between an upper-level jet streak and diabatic processes that influence the development of a low-level jet and a secondary coastal cyclone. *Mon. Wea. Rev.*, **115**, 2227-2261.

INITIAL DISTRIBUTION LIST

		No. Copies
1.	Defense Technical Information Center Cameron Station Alexandria, VA 22304-6145	2
2.	Library, Code 0142 Naval Postgraduate School Monterey, CA 93943-5002	2
3.	Chairman (Code MR/Rd) Department of Meteorolgy Naval Postgraduate School Monterey, CA 93943-5000	1
4.	Chairman (Code OC/Co) Department of Oceanography Naval Postgraduate School Monterey, CA 93943-5000	1
5.	Professor Wendell A. Nuss (Code MR/Nu) Department of Meteorolgy Naval Postgraduate School Monterey, CA 93943-5000	5
6.	Professor Kenneth L. Davidson (Code MR/Ds) Department of Meteorolgy Naval Postgraduate School Monterey, CA 93943-5000	2
7.	Lt. Glen D. Steeley Department Head Class 113 Surface Warfare Officers School Command Newport, RI 02841-5012	2
8.	Director Naval Oceanography Division Naval Observatory 34th and Massachusetts Avenue NW Washington DC 20390	1
9.	Commander Naval Oceanography Command Stennis Space Center, MS 39522-5000	1
10.	Commanding Officer Naval Oceanographic Office Stennis Space Center, MS 39522-5001	1

11. Commanding Officer — 1
Fleet Numerical Oceanography Center
Monterey, CA 93943-5000

12. Commanding Officer — 1
Naval Oceanographic and Atmospheric Research Laboratory
Atmospheric Directorate
Monterey, CA 93943-5000

13. Chief of Naval Research — 1
800 North Quincy Street
Arlington, VA 22217

14. Office of Naval Research — 1
Naval Ocean Research and Development Activity
800 North Quincy Street
Arlington, VA 22217